

## Measurements of Electron Inelastic Mean Free Paths in Materials

J. D. Bourke and C. T. Chantler\*

*School of Physics, University of Melbourne, Parkville, Vic, 3010 Australia*

(Received 10 February 2010; published 20 May 2010)

We present a method for determining inelastic mean free paths (IMFPs) in materials using high-accuracy measurements of x-ray absorption fine structure (XAFS). For electron energies below 100 eV, theoretical predictions have large variability and alternate measurement techniques exhibit significant uncertainties. In this regime, the short IMFP makes photoelectrons ideal for structural determination of surfaces and nanostructures, and measurements are valuable for studies of diverse fields such as low-energy electron diffraction and ballistic electron emission microscopy. Our approach, here applied to solid copper, is unique and exhibits enhanced sensitivity at electron energies below 100 eV. Furthermore, it is readily applicable to any material for which sufficiently high accuracy XAFS data can be obtained.

DOI: [10.1103/PhysRevLett.104.206601](https://doi.org/10.1103/PhysRevLett.104.206601)

PACS numbers: 72.15.Lh, 61.05.cj, 73.50.Gr, 78.70.Dm

The electron inelastic mean free path (IMFP) is the average distance travelled between successive inelastic collisions for an electron moving with a particular energy in a given medium [1]. It is of fundamental importance for a quantitative understanding of electron transport, for electron energy loss spectroscopy and for high-resolution transmission electron microscopy—exciting fields capable of imaging materials at an atomic level [2] and sensitive to changes in interatomic bonding [3]. The mean free path is also crucial for investigations of linear dichroism using photoelectron diffraction [4]; structural investigations using auger electron spectroscopy [5] and x-ray photoelectron spectroscopy [6]; organic semiconductor development for spintronics [7]; and even studying Coulomb explosions triggered by femtosecond x-ray pulses in free-electron lasers [8,9].

However, IMFPs are difficult to determine experimentally, especially at energies below 100 eV–200 eV [10]. As discussed later, different models have predicted large differences in IMFP values in this region, and there has not been a reliable method for assessing the low-energy limits of calculations and predictions which are used for many cognate fields.

Theoretical approaches and computations have large challenges. While theory is well developed for the determination of IMFPs for a free-electron material [11], most solids exhibit complex energy loss functions which require a new approach. It is common to compute IMFPs using experimentally determined optical dielectric functions, or analytic predictive formulae based on these [12]. Empirical curves may also be used when more detailed tabulations are unavailable [13]. These approaches can give applicability at high electron energies, but tend to show discrepancies below 200 eV.

Our work focusses on x-ray absorption fine structure (XAFS) as a solution to this problem. Thousands of papers on XAFS demonstrate its value in probing material struc-

ture down to atomic displacements at the femtometer scale [14]. XAFS theory [15] has shown recent success in the region where it is highly sensitive to the IMFP [16]. We match this theory to experimental XAFS determined by the x-ray extended range technique [17]. This technique provides us with the unprecedented accuracy required to extract the IMFP. In particular, this data is extremely valuable for low-energy electron diffraction (LEED) [18], ballistic electron emission microscopy (BEEM) [19], and experimental configurations where IMFPs for electron energies below 100–200 eV play a role. For much higher electron energies (eg., 200 keV STEM), primary processes will be quite different but secondary scattered photoelectrons may be treated with this new information.

XAFS refers to the complex series of oscillations seen in the photoelectric absorption curve of a material, immediately following an absorption edge. These oscillations convey important structural information about the absorbing material, most notably the relative positions of atoms in the crystal lattice. They are produced by interference between the outgoing photoelectron wave functions from the absorbing atoms, and the returning wave functions back-scattered from atoms in the surrounding region. Since this interference is strongly dependent on the photoelectron energy, the short lifetimes of the photoelectrons cause an energy uncertainty and thus a smearing of the XAFS curve.

The finite IMFP reduces the wave amplitude which diminishes interference (coherence) between the outgoing and incoming waves. Because of the Fourier relationship between the reflected wave function and the resulting XAFS spectrum, this exponential damping leads to a broadening of the XAFS peaks with corresponding energy uncertainty. This effect is particularly clear below 100 eV where the amplitude of the XAFS oscillations is high. To quantify the coherence of the interference, we require knowledge of the photoelectron lifetime or, equivalently, the IMFP.

To obtain the IMFP, we use both experimental and theoretical XAFS. This study focusses on high quality XAFS measurements of copper, for which numerous IMFP predictions are available. Experimental data is taken from Chantler *et al.* [20] and Glover *et al.* [21], whose uncertainties of 0.15%–0.30% are among the lowest in the field. Theoretical data is calculated using the finite difference method (FDM), a development of the finite difference method for near edge structure (FDMNES) [22]. FDMNES uses a cluster calculation where the Schrödinger equation is solved over a finite grid of points to determine the absorption cross section. FDMNES has key advantages of avoiding assumptions about symmetry (used in band-structure approaches) and avoiding muffin-tin approximations (used in multiple-scattering approaches). However, it is computationally expensive, does not implicitly consider the finite photoelectron lifetime, and models an infinite IMFP.

The development of FDM has resolved issues relating to computation time and has generated predictions for the extended XAFS in addition to the near-edge structure. Additionally, it has advantages of requiring no implicit fitting parameters in test cases, and established accuracy near the absorption edge for complicated crystal structures [23]. The approach can then be developed using a point-wise Lorentzian convolution of the calculated XAFS spectrum [16]; by so doing, we uncover the nature of the IMFP at electron energies up to 100–200 eV.

The convolution width is determined using an iterative least squares fitting via the Levenberg-Marquardt method. The procedure includes thermal and core-hole relaxation parameters in addition to the IMFP broadening. Thermal parameters are implemented via an exponential dampening of the XAFS oscillations [16] with known parameters. Figure 1 shows the oscillatory component of the copper spectrum along with four theoretical curves. The first curve shows a direct FDM calculation with no broadening. Subsequent curves demonstrate the effect of adding broadening processes to the model. The finite hole width (or core-hole relaxation width) is a significant contribution near the edge energy, while thermal motion has a negligible effect near-edge but begins to become significant around 30–40 eV above the edge energy. The finite IMFP broadening remains significant over the entire energy range shown, and yields a clear energy-dependent signature.

Processed experimental data for the absolute mass attenuation coefficient for copper in the XAFS region are plotted in Fig. 2, contrasting use of different (semiempirical) IMFP tabulations and predictions. Our approach is clearly sensitive to different theoretical IMFP models, and demonstrates dramatic discrepancies between current theories at low energies. The need for a more realistic model for the IMFP below 30–40 eV is also clear, where alternate theories lead to XAFS that are severely discrepant with the experimental data.

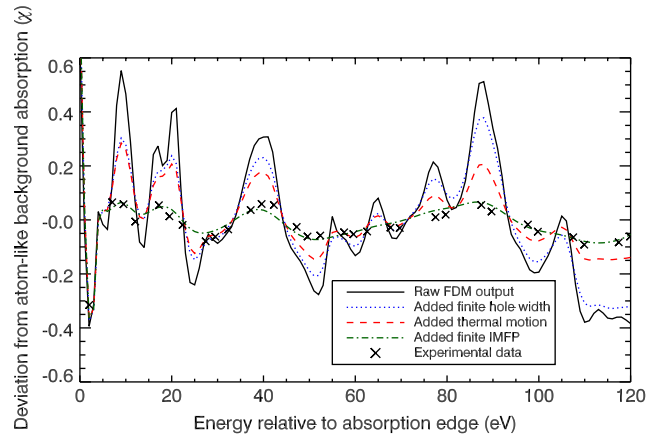


FIG. 1 (color online). Oscillatory component ( $\chi$ ) of copper XAFS as determined by FDM, illustrating the results of progressively including broadening processes. The finite core-hole relaxation width produced by the loss of the photoelectron from the absorbing atom is most significant just above the edge. Oscillations are damped due to the well-understood thermal vibrations present at room temperature. Finally, the finite IMFP remains significant across the plotted energy range. The oscillatory component of the experimental data is shown for comparison, and clearly is accounted for by including all theoretical contributions.

At higher energies, thermal broadening becomes more dominant and the sensitivity to IMFP broadening decreases and becomes less incisive. Further, the atomlike background absorption has a near-edge offset that becomes nonlinear and difficult to quantify over a sufficiently large (and material-dependent) energy range [24]. These concerns place a practical upper limit on the energy range of our analysis which, for this case, is around 120 eV. Improved understanding of the near-edge offset combined with enhanced statistical data sets and a low temperature

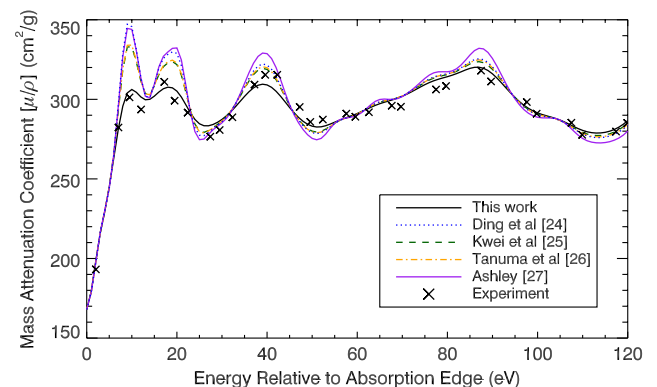


FIG. 2 (color online). Mass attenuation coefficients for copper calculated using different tabulations for the IMFP described in the text. The data are particularly sensitive to the choice of IMFP at energies within 30–40 eV of the absorption edge. Current IMFP predictions yield XAFS strongly inconsistent with experiment in this region.

measurement could in principle, however, yield a rough upper limit as high as 500 eV for elemental copper. This limit is naturally material dependent.

Figure 3 shows our extracted IMFPs with plotted 3 standard deviation uncertainties, following our fitting procedure and the propagation of uncertainties from experimental error bars. Also shown are theoretical IMFPs predicted by Ding *et al.* [25], Kwei *et al.* [26], Tanuma *et al.* [27] and Ashley [28], based on the optical data model presented by Penn [11]. The results of Kwei *et al.* provide closest agreement with our current work. Their approach used a representation of the optical dielectric function as a summation of extended Drude terms, enabling an elegant extension of the experimentally-determined dielectric function to the regime of finite momentum transfer. Such an extension is required by all optical data models, but is often accomplished with a single pole representation of the dielectric function which is much less suited to lower electron energies. Tanuma *et al.* use a different multiple-pole representation below 200 eV, and produce results at least approaching our current measurements. Their tabulation is particularly useful due to its larger implemented energy range.

Inspection of our uncertainties demonstrates the importance of high-accuracy XAFS measurements: greater input experimental uncertainties would yield substantially larger IMFP uncertainty, in turn yielding less incisive results. A feature of particular interest is the form of the IMFP as we approach zero photoelectron energy. Current theory predicts that the IMFP approach infinity in this limit. However, the rate at which this occurs and the position of the minimum IMFP are not established. For copper, the position of the minimum is given variously as  $\sim 65$  eV

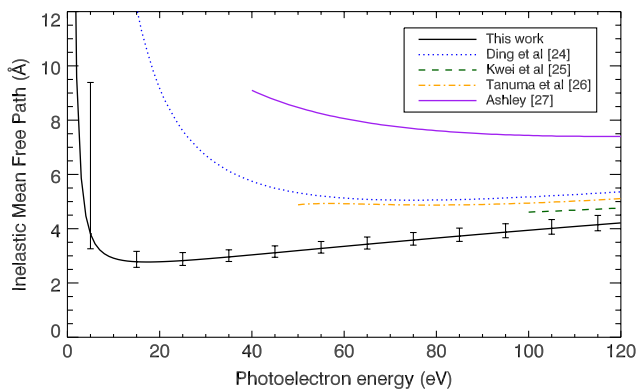


FIG. 3 (color online). The inelastic mean free path (IMFP) for copper metal as determined from x-ray absorption fine structure (XAFS) with 3 standard deviation error bars, compared with theoretical predictions of the IMFP. Significant deviation is clear as the energy drops below 100 eV. Although data is not available from the multiple-pole calculation of Kwei *et al.* in this region, it can be seen that their approach is more consistent than alternatives as we approach 100 eV. At lower energies, the IMFP appears much lower than previously predicted.

[29],  $\sim 80$  eV [27,30], and  $\sim 100$  eV [31]. Note that none of these authors claim accuracy below 100 eV. Our results show a significant deviation in this position, and also in the shape of the IMFP curve. We predict a smooth decline with an abrupt turning point at around 17 eV, in contrast with the broad minima commonly seen in alternate theories. Below 1–5 eV, the asymptotic behavior of the IMFP means that competing processes such as the core-hole relaxation will make the IMFP effectively unobservable. The approach detailed here severely constrains the low-energy limit by accurate, high precision measurements and rigorous implementation of known (broadening) processes.

The variation in current theoretical treatments raises questions about theoretical extension to less ideal materials than elemental copper. The refinements of Kwei *et al.* of the single pole data model certainly yield improved agreement with our analysis. However, all available theories still employ limiting assumptions about the dependence of the optical dielectric function on momentum transfer, and are often reliant on experimental optical data. Many authors, including Kwei *et al.* and Tanuma *et al.*, use sum-rule checks to verify the experimental optical data over a range of energies. This is a valuable analysis tool, however it does not guarantee consistency of the optical energy loss function over small energy ranges (e.g., Fig. 15 of [29]). This leads to concerns over the applicability of such theories to more complicated media, even for moderately simple binary compounds. Conversely, the experimental XAFS approach is well defined for arbitrary systems, and is potentially applicable to complex materials.

So with the new accurate experimental approaches, and with reliable XAFS theory, our method can take any experimental XAFS spectrum, use known thermal effects and parameters including sample temperature, and generate measurements of the inelastic mean free path of the photoelectron in that material. The figures show convolution widths of order 1–10 eV, in the range of energies up to 100–200 eV above any absorption edge, represent inelastic mean free paths from approximately 2 Å to 10–12 Å. These photoelectrons are probing a local nanoenvironment. Depending upon the x-ray energies chosen, they can either probe narrow surface structure at the nanolevel, or they can investigate the environment around active elements or ions of interest.

For example, some kind of complex enzyme might have an active copper center crucial for its activity. This method can probe the site and the mean free path in the local region, some few nanometers around the site. Alternatively, a quantum well made by a single copper, silver, or gold atom, embedded in a diamond or silicon lattice as part of a quantum measurement or electronic circuit, can be investigated. Particular regions of complex nanolayers can be probed for electron mean free paths and other structural details around particular features.

In recent work this has raised the important issue of localization in inelastic scattering in nonelemental compounds. If the scattering is local, there exists a short IMFP

compared with interatomic distances, and very good and relatively simple predictions can be made on the basis of a product of component cross sections from the impact factor. This also implies that the IMFP experimental data can be used efficiently. If however the scattering is non-local, as in the case of far-reaching IMFPs, then the computation is quite complex and it is not straightforward to derive the scattering cross section of a molecule from individual elemental IMFPs [2]. A classic paper [32] has explained why obtaining such surface sensitivities for electron spectroscopies is important and that the need is widespread. This opportunity will also provide information for the optimization of beam characteristics for high nano-scale resolution.

Low accuracy data sets for our technique could be obtained on biological species in hours or less, while high-accuracy measurements can require several days. Data analysis can extract IMFPs within days, but can be dramatically hastened with a routine system. The principal requirement is a high density of data points, which requires highly accurate energy measurements.

Derivation of the IMFP assists much more than just the interpretation of nanoenvironments using x rays. LEED depends upon these photoelectron transport parameters, with particular discrepancies to current theories being reported between 100 eV–200 eV [18]. BEEM is also sensitive to inelastic losses at very low energies, and has lead to determinations of attenuation lengths at energies as low as a few eV [19]. The results from BEEM are qualitatively consistent with our work, despite measuring a different parameter due to elastic contributions.

We have presented an approach for measuring IMFPs particularly incisive in the low-energy regime. Inelastic mean free paths are valuable for applications including XPS, AES, LEED and BEEM, and also to discriminate between different theoretical approaches. The approach is readily applicable to any material for which good accuracy XAFS data can be obtained and is applicable to x-ray and electron experimental paradigms.

The authors acknowledge Y. Joly and J. L. Glover in our developments with FDMNES, and the experimental teams who measured our high accuracy XAFS data. We also acknowledge the ASRP for providing the funding for the experimental data used in this research.

---

\*chantler@unimelb.edu.au

- [1] C.J. Powell and A. Jablonski, *Nucl. Instrum. Methods Phys. Res., Sect. A* **601**, 54 (2009).
- [2] K. Kimoto, T. Asaka, M. Saito, Y. Matsui, and K. Ishizuka, *Nature (London)* **450**, 702 (2007).
- [3] D. A. Muller, L. F. Kourkoutis, M. Murfitt, J. H. Song, H. Y. Hwang, J. Silcox, N. Dellby, and O. L. Krivanek, *Science* **319**, 1073 (2008).
- [4] F. U. Hillebrecht, H. B. Rose, T. Kinoshita, Y. U. Idzerda, G. van der Laan, R. Denecke, and L. Ley, *Phys. Rev. Lett.* **75**, 2883 (1995).
- [5] W. S. M. Werner, W. Smekal, H. Stori, H. Winter, G. Stefani, A. Ruocco, F. Offi, R. Gotter, A. Morgante, and F. Tommasini, *Phys. Rev. Lett.* **94**, 038302 (2005).
- [6] P. J. Cumpson, *Surf. Interface Anal.* **25**, 447 (1997).
- [7] M. Cinchetti, K. Heimer, J.-P. Wstenberg, O. Andreyev, M. Bauer, S. Lach, C. Ziegler, Y. Gao, and M. Aeschlimann, *Nature Mater.* **8**, 115 (2009).
- [8] Z. Jurek, G. Faigel, and M. Tegze, *Eur. Phys. J. D* **29**, 217 (2004).
- [9] R. Neutze, R. Wouts, D. van der Spoel, E. Weckert, and J. Hajdu, *Nature (London)* **406**, 752 (2000).
- [10] D. P. Pappas, K.-P. Kamper, B. P. Miller, H. Hopster, D. E. Fowler, C. R. Brundle, A. C. Luntz, and Z.-X. Shen, *Phys. Rev. Lett.* **66**, 504 (1991).
- [11] D. R. Penn, *Phys. Rev. B* **35**, 482 (1987).
- [12] C. J. Powell and A. Jablonski, *J. Phys. Chem. Ref. Data* **28**, 19 (1999).
- [13] M. P. Seah and W. A. Dench, *Surf. Interface Anal.* **1**, 2 (1979).
- [14] R. F. Pettifer, O. Mathon, S. Pascarelli, M. D. Cooke, and M. R. J. Gibbs, *Nature (London)* **435**, 78 (2005).
- [15] J. J. Rehr and R. C. Albers, *Rev. Mod. Phys.* **72**, 621 (2000).
- [16] J. D. Bourke, C. T. Chantler, and C. Witte, *Phys. Lett. A* **360**, 702 (2007).
- [17] C. T. Chantler, *Eur. Phys. J. Special Topics* **169**, 147 (2009).
- [18] J. Rundgren, *Phys. Rev. B* **59**, 5106 (1999).
- [19] R. P. Lu, B. A. Morgan, K. L. Kavanagh, C. J. Powell, P. J. Chen, F. G. Serpa, and W. F. Egelhoff, Jr., *J. Appl. Phys.* **87**, 5164 (2000).
- [20] C. T. Chantler, C. Q. Tran, Z. Barnea, D. Paterson, D. Cookson, and D. X. Balaic, *Phys. Rev. A* **64**, 062506 (2001).
- [21] J. L. Glover, C. T. Chantler, Z. Barnea, N. A. Rae, C. Q. Tran, D. C. Creagh, D. Paterson, and B. B. Dhal, *Phys. Rev. A* **78**, 052902 (2008).
- [22] Y. Joly, *Phys. Rev. B* **63**, 125120 (2001).
- [23] J. L. Glover, C. T. Chantler, A. V. Soldatov, G. Smolentsev, and M. C. Feiters, *AIP Conf. Proc.* **882**, 625 (2007).
- [24] J. D. Bourke and C. T. Chantler, *Nucl. Instrum. Methods Phys. Res., Sect. A* (2010, in press).
- [25] Z.-J. Ding and R. Shimizu, *Surf. Sci.* **222**, 313 (1989).
- [26] C. M. Kwei, Y. F. Chen, C. J. Tung, and J. P. Wang, *Surf. Sci.* **293**, 202 (1993).
- [27] S. Tanuma, C. J. Powell, and D. R. Penn, *Surf. Interface Anal.* **17**, 911 (1991).
- [28] J. C. Ashley, *J. Electron Spectrosc. Relat. Phenom.* **50**, 323 (1990).
- [29] W. S. M. Werner, K. Glantschnig, and C. Ambrosch-Draxl, *J. Phys. Chem. Ref. Data* **38**, 1013 (2009).
- [30] S. F. Mao, Y. G. Li, R. G. Zeng, and Z. J. Ding, *J. Appl. Phys.* **104**, 114907 (2008).
- [31] J. M. Fernandez-Varea, F. Salvat, M. Dingfelder, and D. Liljequist, *Nucl. Instrum. Methods Phys. Res., Sect. B* **229**, 187 (2005).
- [32] C. J. Powell, *J. Electron Spectrosc. Relat. Phenom.* **47**, 197 (1988).